Journal of the Physical Society of Japan **83**, 014705 (2014)
http://dx.doi.org/10.7566/JPSJ.83.014705

Spin-Polarized Angle-Resolved Photoelectron Spectroscopy of the So-Predicted Kondo Topological Insulator SmB_6

Shigemasa Suga[1,2*], Kazuyuki Sakamoto[3], Taichi Okuda[4], Koji Miyamoto[4], Kenta Kuroda[5], Akira Sekiyama[6], Junichi Yamaguchi[6], Hidenori Fujiwara[6], Akinori Irizawa[1], Takahiro Ito[7†], Shinichi Kimura[7‡], T. Balashov[8], W. Wulfhekel[8], S. Yeo[9], Fumitoshi Iga[10], and Shin Imada[11]

[1]*Institute of Scientific and Industrial Research, Osaka University, Ibaraki, Osaka 567-0047, Japan*
[2]*Max-Planck-Institute for Microstructure Physics, Weinberg 2, Halle 06120, Germany*
[3]*Department of Nanomaterials Science, Chiba University, Chiba 263-8522, Japan*
[4]*Hiroshima Synchrotron Radiation Center, Hiroshima University, Higashihiroshima, Hiroshima 739-0046, Japan*
[5]*Graduate School of Science, Hiroshima University, Higashihiroshima, Hiroshima 739-8526, Japan*
[6]*Graduate School of Engineering Science, Osaka University, Toyonaka, Osaka 560-8531, Japan*
[7]*UVSOR, Institute for Molecular Science, Okazaki, Aichi 444-8585, Japan*
[8]*Physikalisches Institut, Karlsruhe Institute of Technology, 76131 Karlsruhe, Germany*
[9]*Korea Atomic Energy Research Institute, Daejeon 305-600, Republic of Korea*
[10]*Faculty of Science, Ibaraki University, Mito 310-0056, Japan*
[11]*Department of Physical Sciences, College of Science and Engineering, Ritsumeikan University, Kusatsu, Shiga 525-8577, Japan*

(Received September 4, 2013; accepted October 22, 2013; published online December 10, 2013)

Undoped and slightly Eu-doped SmB_6 samples show the opening of a gap with decreasing temperature below ~150 K. The spectral shapes near the Fermi level (E_F) at 15 K have shown a marked increase in intensity of the peak at a binding energy (E_B) of approximately 12 meV with decreasing photon energy ($h\nu$) from 17 to 7 eV. Angle-resolved spectra of SmB_6 measured at $h\nu = 35$ eV just after the in situ cleavage showed clear dispersions of several bands in the E_B region from E_F to 4 eV. Spin-polarized photoelectron spectra were then measured at 12 K and a light incidence angle of ~50°. In contrast to the lack of spin polarization for the linearly polarized light excitation, clear spin polarization was observed in the case of circularly polarized light excitation. The two prominent peaks at $E_B \sim 12$ and ~150 meV have shown opposite signs of spin polarization which are reversed when the helicity of the light is reversed. The sign and magnitude of spin polarization are consistent with a theoretical prediction for the $^6H_{5/2}$ and $^6H_{7/2}$ states.

1. Introduction

SmB_6 is known to show a gap opening at low temperatures below ~150 K,[1,2] while it is a mixed valence metallic material above this temperature. Although a Kondo semiconductor scenario was proposed for this material as well as for YbB_{12} systems at low temperatures,[3,4] the different behaviors of the change in the spectral shapes between these two materials were experimentally clarified.[5] Very recently, the possibility of a topological insulator scenario has been theoretically proposed for SmB_6.[6,7] In parallel, intensive studies of angle-resolved photoelectron spectroscopy (ARPES) are going on in several groups.[8–12] Efforts are also being made for spin-polarized angle-resolved photoelectron spectroscopy (SP-ARPES) of SmB_6.

Clarification of the surface and bulk electronic structure is quite important in such a study because the surface electronic structure is often very different from the bulk electronic structure in most lanthanide compounds. The photon energy ($h\nu$)-dependent study is powerful for this purpose owing to the variation of the probing depth from the sample surface with $h\nu$ (or kinetic energy E_K) and the $h\nu$ dependence of the photoionization cross section (PICS) of different orbitals. In addition, full utilization of the circularly and linearly polarized light is powerful for discussion on the origin of the observed spin polarization of photoelectrons.[13,14]

2. Experimental Methods

The angle-integrated photoelectron spectra of $Sm_{0.85}Eu_{0.15}B_6$ and SmB_6 were measured on fractured surfaces at temperatures between 200 and 15 K at BL7U of UVSOR-II by using a linearly polarized light with p-polarization. Many tiny specular cleaved regions as well as nonspecular rough surface regions coexisted on this fractured clean surface within a beam spot size of few hundred μm. Measurement was performed at $h\nu$ between 17 and 7 eV by using an MBS A-1 hemispherical analyzer. The acceptance angle along the entrance slit of the analyzer was 14°.

The angle-resolved spectra (ARPES) of SmB_6 were measured at BL-9B of HiSOR at temperatures between 40 and 12 K by using a circularly polarized synchrotron radiation (SR) light at $h\nu \sim 35$ eV with the $h\nu$ resolution of 20 meV on a cleaved (100) surface. A single crystalline SmB_6 was fixed in a drilled hole of the sample holder using conductive epoxy (Muromacbond). By means of a pinpost cleaving of a single-crystal sample with dimensions of $1 \times 1 \times 2\,mm^3$, a specularly cleaved region with a scale of ~0.5 mm was obtained at 82 K under a vacuum of $\sim 4 \times 10^{-8}$ Pa in the analyzer chamber, in which the cleaved sample was further cooled down to 40–12 K under a vacuum of 8×10^{-9} Pa (at 12 K). The measurement was performed by use of a SCIENTA R4000 hemispherical analyzer modified for spin-polarized photoemission with the analyzer energy resolution set to 19 meV. The SR was incident onto the SmB_6 at ~50° from its surface normal.

For SP-ARPES, the analyzer resolution was set to 40 meV and the acceptance angle along the slit was set to 1.5°. The spin polarization was measured for photoelectrons emitted ~3° off the surface normal by use of an Fe–O VLEED spin detector[15,16] for the σ^+ and σ^- circularly polarized light as well as horizontally and vertically polarized light, as illustrated in Fig. 1. The degree of the spin polarization was

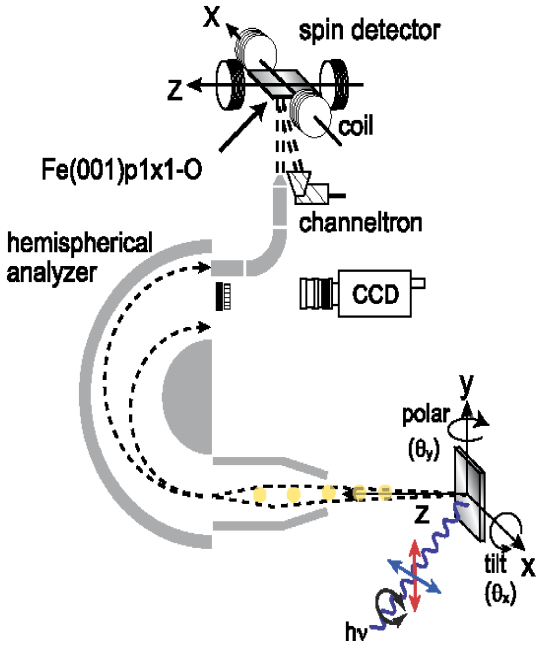

Fig. 1. (Color online) Experimental setup for spin-polarized angle-resolved photoelectron spectroscopy at BL-9B of HiSOR. The light was incident in the x–z plane and the incidence angle was set to ∼50° from the z-direction in the case of normal photoemission.

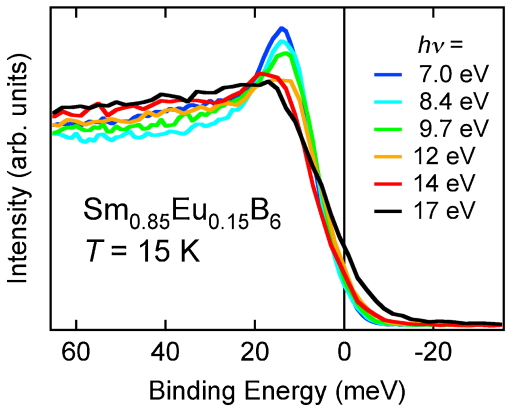

Fig. 2. (Color online) Angle-integrated photoelectron spectra of $Sm_{0.85}Eu_{0.15}B_6$ measured at 15 K between $h\nu = 17$ and 7 eV.

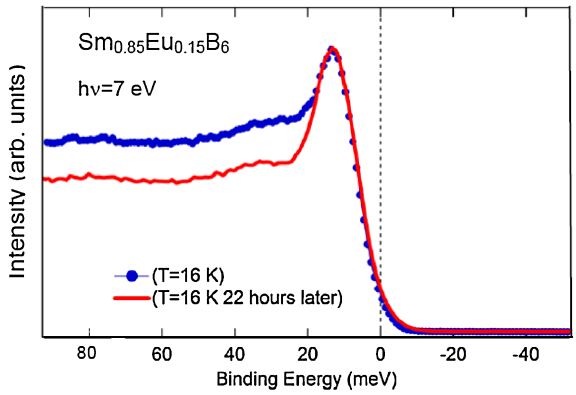

Fig. 3. (Color online) Change of the angle-integrated spectra of $Sm_{0.85}Eu_{0.15}B_6$ with time measured at $h\nu = 7$ eV and 16 K under a vacuum of 5×10^{-8} Pa.

evaluated by changing the direction of the remanent magnetization of the Fe of this spin detector by reversing the current through a coil, as shown in Fig. 1. The incidence angle of the emitted photoelectron from SmB_6 onto the Fe–O spin detector was set to ∼6.5° from the Fe–O surface-normal and the incident electron energy was decelerated down to ∼6 eV. The diffracted electron intensity was measured by using a channeltron. After SP-ARPES measurement, the sample was once retracted to the sample preparation chamber and exposed to a vacuum of 2×10^{-7} Pa for 20 min and again transferred back into the analyzer chamber where the angle-resolved spectra were measured again to check the surface contamination effect on the band dispersions.

3. Results

3.1 Angle-integrated spectra

First, the $h\nu$ dependence of the results of $Sm_{0.85}Eu_{0.15}B_6$ is described. The behavior of the angle-integrated spectra with the change in temperature between ∼200 and 10 K was rather similar between this material and SmB_6 except for the absolute E_B of the peak structure (not shown). Figure 2 shows the $h\nu$ dependence of the spectra near E_F of $Sm_{0.85}Eu_{0.15}B_6$ measured at 15 K between $h\nu = 17$ and 7 eV with the total energy resolution ΔE_K in the range from 17 to 9 meV. Gradual change in spectral shape with $h\nu$ is recognized. A prominent peak is observed for $h\nu < 10$ eV at $E_B \sim 12$ meV.

Figure 3 shows the spectrum of $Sm_{0.85}Eu_{0.15}B_6$ at $h\nu = 7$ eV and 16 K just after the fracturing under 5×10^{-8} Pa at BL7U of UVSOR-II and the spectrum of the same surface measured 22 h after the fracturing under continuous radiation from SR. The two spectra are tentatively normalized at the peak for a simple comparison. If the background is subtracted in the region up to 80 meV from the spectra in Fig. 3, the ∼12 meV peak is noticeably enhanced relative to the intensity at $E_B > 20$ meV with time.

3.2 Angle-resolved spectra

The E_B–$k_\parallel$ intensity plot of the ARPES spectra measured at BL-9B of HiSOR at 35 eV and 30 K on a cleaved (001) surface is shown in Fig. 4. Figures 4(a) and 4(b) show the ARPES spectra and its second energy derivative, respectively, in the E_B range from E_F to 6 eV measured just a few minutes after the cleavage. The white regions in the spectrum (a) and the dark regions in the second energy derivative (b) correspond to the region with high photoemission intensity. The abscissa $k_\parallel$ is the k value along the (100) direction. The normal emission at $h\nu = 35$ eV corresponds to k_z in the middle region between the $\Gamma(0, 0, 0)$ and $X(0, 0, \pi/a)$.[9)]

A clear doublet with almost negligible dispersion is observed near E_F within $E_B < 200$ meV. In addition, dispersing bands are observed within 2 eV from E_F as recognized in Figs. 4(a) and 4(b). Here, a band with a bottom (or maximum E_B) at $E_B \sim 1.7$ eV near ~ 0 Å^{-1} is clearly resolved. Furthermore, a slightly dispersing band is recognized around $E_B \sim 0.6$ eV near ~ 0 Å^{-1}. An additional band is also recognized at approximately $E_B \sim 0.6$ eV in the vicinity of $k_\parallel \sim -0.6$ Å^{-1}. Moreover, a dispersing band is observed between 2.5 and 3.5 eV with a top (minimum E_B) near $k_\parallel \sim -0.6$ Å^{-1}.

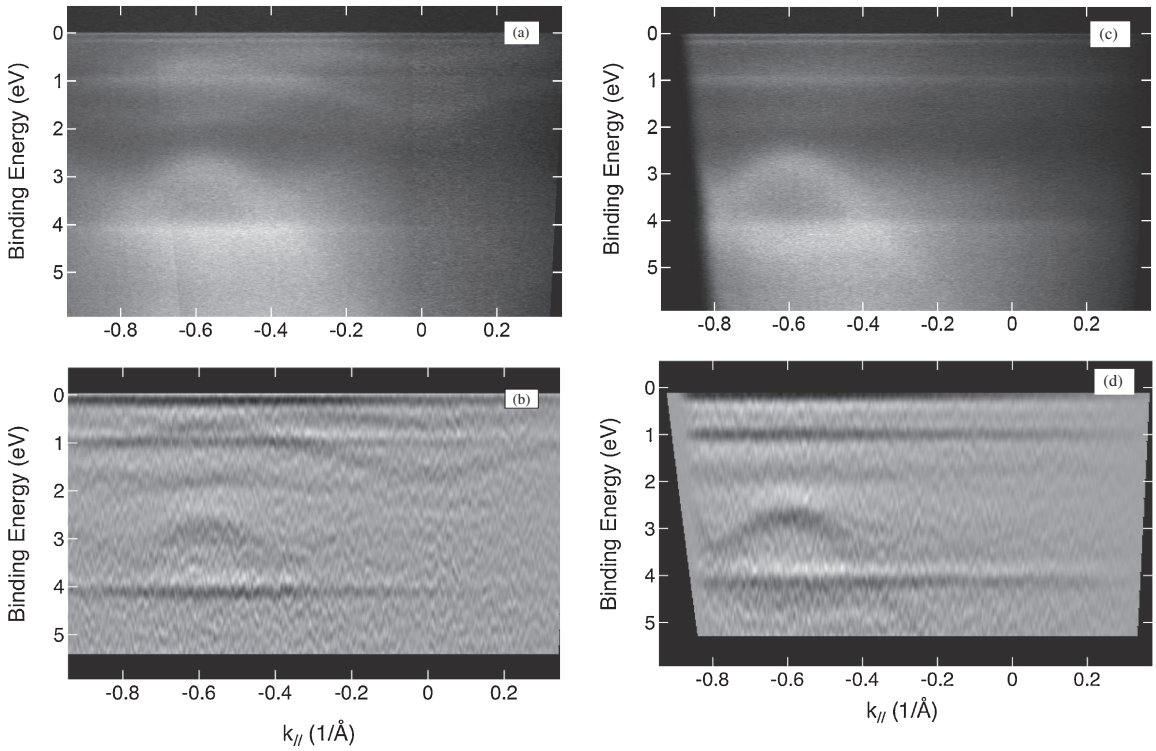

Fig. 4. Angle-resolved photoemission spectra of SmB_6 measured at $h\nu = 35$ eV at 12 K parallel to the $(0,0,0)$–$(\pi/a,0,0)$ direction (or surface $\bar{\Gamma}$–$\bar{X}$ direction). (a) and (b) are the raw spectrum and second energy derivative just after cleavage, respectively. (c) and (d) are those after 1 h under a vacuum of $\sim 1 \times 10^{-8}$ Pa, respectively.

Figures 4(c) and 4(d) show the corresponding results measured half an hour after the measurement (a) on the same sample surface. Here, the dispersing bands and structures between 0.5 and 2 eV are no longer recognized in the ARPES spectrum, whereas the dispersing band between 2.5 and 3.5 eV is still observed as before.

4. Spin-Polarized and Angle-Resolved Photoelectron Spectra

The emitted photoelectrons from SmB_6 at 12 K were accepted within 1.5° along the slit and guided to the Fe–O VLEED spin detector[15,16] and SP-ARPES spectra were measured by reversing the magnetization direction of the Fe–O spin detector along the x-direction shown in Fig. 1. The spin polarization was measured parallel to the x-direction for the circularly polarized light excitation in Figs. 5(a) and 5(b). The results for linearly polarized excitation are shown in Figs. 5(c) and 5(d). These single channel SP-ARPES measurements were performed at 3° off the surface normal direction to cover the $k_{\|}y$ region between $\sim$0.11 and $\sim$0.18 Å^{-1} to try to observe the possible spin polarization of the surface electron pocket around the $\bar{\Gamma}$ point near E_F with the least broadening, although the surface states were reported to be rather weak and broad.[10–12] The pass energy of the analyzer was set to 5 eV, but the resolutions of both the photon monochromator and the electron energy analyzer were broadened twice to have a higher counting rate. Then, the energy resolution (FWHM) was set as $\sim$50 meV for these SP-ARPES measurements.

Figures 5(a)–5(d) show the results for the σ^+ and σ^- circularly polarized lights as well as for the vertical and horizontal linearly polarized lights, respectively. The measuring time to obtain each result [(a) to (d)] was between 30 min and 1 h. Two peaks are clearly observed in the E_B from E_F to 0.2 eV. As observed for the σ^+ polarization excitation (a), the two peaks show opposite signs of spin polarization with a negative sign for the peak near $E_B = 10$–40 meV and a positive sign for the second peak at $E_B \sim 150$–160 meV. The magnitude of spin polarization is approximately -0.40 for the first peak and $+0.20$ for the second peak.

Since the spin polarization was estimated by $P_s = (I\uparrow - I\downarrow)/(I\uparrow + I\downarrow)$ in Figs. 5(a)–5(d), the contributions of the background from the non-4f state may influence the experimentally evaluated P_s. If one can neglect the spin polarization of the background, P_s might be evaluated as -0.42 and 0.28, respectively, after subtracting the background in Fig. 5(a). When the helicity of the excitation light is switched to σ^-, the polarization of the first peak shows a positive sign and that of the second peak shows a negative sign. Namely, their magnitude is 0.50 and -0.25, respectively. After subtracting the background contribution, P_s became 0.57 and -0.34, respectively. The difference in the absolute value of the polarization for the σ^+ and σ^- may be mostly due to the possible difference in the circular polarization of the incident light, which is not accurately calibrated for this experiment. Then, the spin polarization P_ss will be represented by the average values as 0.50 and 0.31 with opposite signs for the two peaks. When the polarization of the excitation light was switched to linearly polarized light, no spin polarization was observed not only for the two prominent peaks but also in the smaller E_B region down to $E_B = 0$ eV, where the surface states around the $\bar{\Gamma}$ point are expected. After the full set of spin-polarized angle-resolved photoelectron measurements, the spin-integrated ARPES

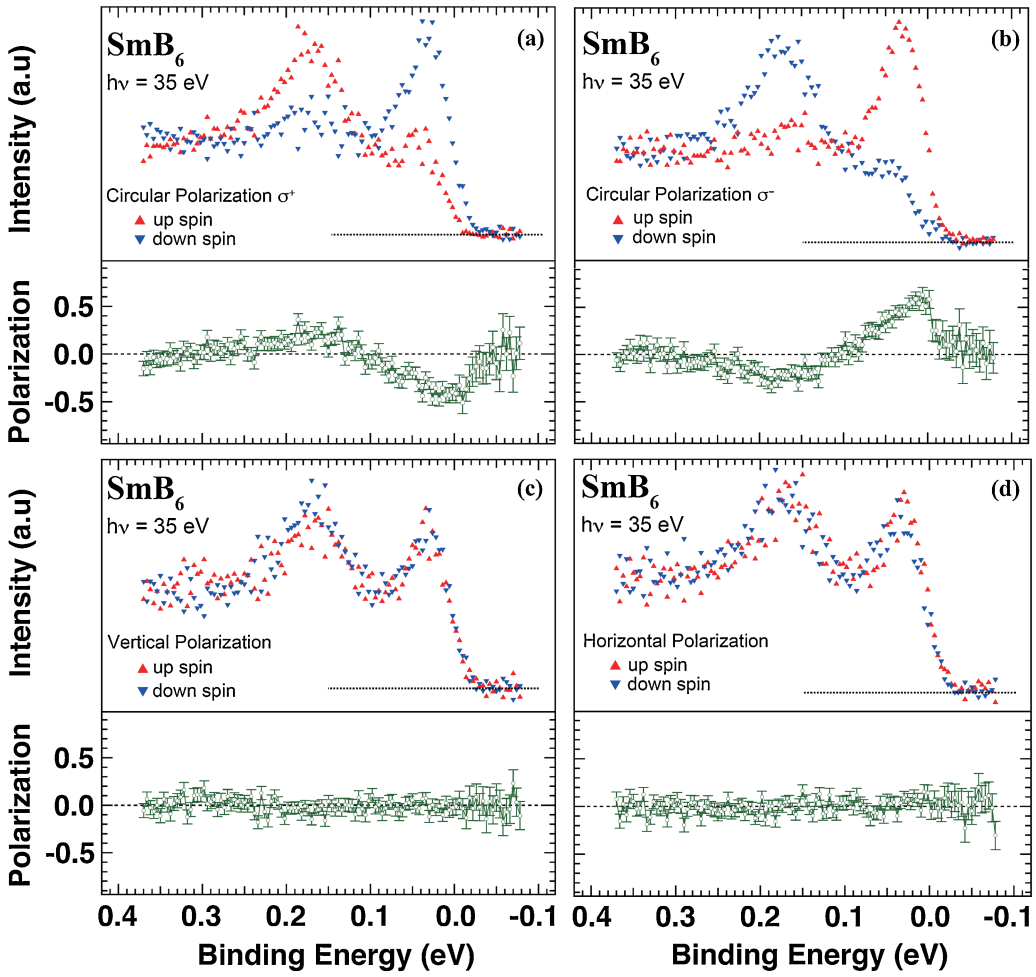

Fig. 5. (Color online) Spin-polarized and angle-resolved photoelectron spectra measured at 12 K and $h\nu = 35$ eV after the measurement shown in Fig. 4(b). σ^+, σ^-, linearly polarized light excitations for the spectra (a)–(d). The intensity is given in an arbitrary unit (a.u). The spin parallel to the x-axis in Fig. 1 was observed for the circularly polarized light excitation. Spin polarization was not observed for the linearly polarized light excitation.

measurement was performed again, where the spectra were found to be not essentially changed in the 4 h before and after the SP-ARPES measurement.

5. Discussion

The $h\nu$ dependence of the angle integrated spectra shown in Fig. 2 is first discussed. The prominent peak detected at 12 meV at $h\nu = 7$ eV is weakened with increasing $h\nu$ at the temperature of 15 K. The observed behavior of this peak near E_F is most likely due to the $h\nu$ dependence of the photoionization cross section (PICS) or matrix element effect, as explained later. As already reported, the gap opens at E_F below ~150 K.[5] As for the temperature dependence of the spectra at $h\nu = 7$ eV (not shown here), the peak closest to E_F in $Sm_{0.85}Eu_{0.15}B_6$ becomes sharper and its peak energy decreases gradually from 24 meV at 200 K to 12 meV at 15 K, as if the spectral weight shifts to a lower (smaller) E_B with decreasing temperature. In SmB_6, a similar temperature dependence is observed. Namely, the peak shifts from 29 meV at 200 K to 18 meV at 15 K at $h\nu = 8.4$ eV.[5] A very similar temperature dependence was clearly observed in the bulk-sensitive Sm 4f spectral weight measured at $h\nu \sim 8$ keV [Fig. 1 of Ref. 5]. The shift of the peak in the spectra at $h\nu = 7$ and 8.4 eV correlates strongly with the temperature dependence of the Sm 4f states probed at $h\nu \sim 8$ keV.

When $h\nu$ decreases from 80 to 7 eV, for example, the PICS of the Sm 4f state decreases markedly with $h\nu$.[17] Although the PICS of the Sm 4f states is one order of magnitude larger than that of the Sm 5d states at 80 eV, it becomes comparable to or slightly lower than that of the Sm 5d states below $h\nu \sim 27$ eV as judged from the PICSs of La 5d and Gd 5d states.[17] The Sm 4f PICS becomes much lower than those of the Sm 5d and B 2sp states for $h\nu < 17$ eV. The PICS of the Sm 4f states is still larger than that of the Sm 5d states at $h\nu = 35$ eV and more than three times larger than that of the B 2sp states above $h\nu = 40$ eV. The peak observed in Fig. 2 for $h\nu < 17$ eV is therefore not dominated by the Sm 4f spectral weight but is due to the hybridized states between the B 2sp, Sm 5d, and Sm 4f states. The smaller value of E_B of the peak in $Sm_{0.85}Eu_{0.15}B_6$ at low temperatures than that in SmB_6 at the same temperature and $h\nu$ is in accordance with the smaller degree of Sm 4f-conduction band (B 2sp and Sm 5d) hybridization accompanied by the smaller gap opening than in SmB_6.[18]

It is noticed in Fig. 3 that the PES intensity of $Sm_{0.85}Eu_{0.15}B_6$ measured at $h\nu = 7$ eV and 16 K decreases relatively above $E_B \sim 25$ meV after 22 h in the vacuum of 5×10^{-8} Pa. Although not shown here, the PES spectral shape of this material at $h\nu = 17$ eV shows very similar behavior at 14 K after 26 h. Such results are hardly explicable by the PICS

effect. A more plausible interpretation is that the electronic structures with $E_B > 20$ meV at low temperatures are largely suppressed with time with a possible change in surface quality, while the peak of the bulk origin is not markedly suppressed. The comparison of the results in Figs. 4(a) and 4(c) confirms this interpretation as well. Namely, surface-derived states are gradually suppressed with time on the surface of fractured or cleaved $Sm_{0.85}Eu_{0.15}B_6$ and SmB_6.

In-gap surface states in the hybridization gap in the Kondo insulator SmB_6 at low temperatures have recently been analyzed by high energy resolution ARPES[10–12] in the vicinity of E_F. The electric resistivity behavior at low temperatures was ascribed to the in-gap states crossing E_F. The negligible k_z dependence suggests the surface origin of these in-gap states. In-gap metallic surface states with noticeable dispersions were reported around the surface $\bar{X}$ and $\bar{\Gamma}$ points.[10–12] Rather large oval-shaped Fermi surfaces were observed around the $\bar{X}$ point.[10] The in-gap metallic surface states around the $\bar{\Gamma}$ point were much weaker in the first Brillouin zone (BZ) than in the second BZ at $h\nu = 25$ eV.[10] The two prominent peaks observed in Figs. 4(a) and 4(c) at $E_B \sim 12$ and $\sim$150 meV are ascribable to the $^6H_{5/2}$ and $^6H_{7/2}$ final states, respectively. Although these states resulting from the Sm 4f states are clearly resolved in both Figs. 4(a) and 4(c), the in-gap metallic surface states are not resolved even in Figs. 4(b) and 4(d) possibly owing to their low intensity on the surface presently investigated and the selection of the photon energy ($h\nu = 35$ eV) in this experiment, though the wave number k_F crossing E_F was reported to stay almost constant irrespective of $h\nu$.[10–12]

Although the time dependence or surface condition dependence of the spectral shapes was not discussed in Refs. 10–12, such a dependence was carefully checked and analyzed in Ref. 19 at $h\nu = 21.2$ eV, where time evolution of ARPES spectra along $\bar{M}$–$\bar{\Gamma}$–$\bar{M}$ at 6 K under 5×10^{-9} Pa was presented. The nonmetallic dispersing bands around the $\bar{\Gamma}$ point with their bottoms at $E_B \sim 1.7$ and 2.3 eV in Fig. 4(b) are also reported in Ref. 19. In our experiment, these dispersive bands observed in Fig. 4(b) are no longer observed in Fig. 4(d) half an hour after the measurement shown in Figs. 4(a) and 4(b) and can be ascribed to surface states. Although a polarity-driven origin was proposed for the B-2p metallic surface state derived from the B_6 terminated SmB_6 surface near the $\bar{\Gamma}$ point,[12] we could not observe such metallic surface states on our sample surface possibly due to the difference in the surface quality or photon energy ($h\nu = 35$ eV).

Now, the SP-ARPES results are discussed. Since the PICS of the Sm 4f states is noticeably larger than those of the Sm 5d and B 2sp states at $h\nu = 35$ eV, the two peaks observed in Fig. 5 are understood to correspond mainly to the Sm 4f-dominated $^6H_{5/2}$ (smaller E_B) and $^6H_{7/2}$ final states. Let ℓ and ℓ' indicate the azimuthal quantum numbers of the electron before and after the photoexcitation, respectively. According to the dipole excitation, it is known that $\ell' = \ell \pm 1$. In the present case, ℓ is considered to be 3 and the photoelectron has either $\ell' = 2$ or 4. It has been predicted for the photoexcitation of Ce 4f electrons by photons of 40.8 eV that the photoexcitation probability to the $\ell' = 4$ state is much larger (by more than several times) than that to the $\ell' = 2$ state.[20] Therefore, we suppose that Sm 4f electrons are mostly excited as photoelectrons with $\ell' = 4$.

Circularly polarized light with σ^+ (σ^-) polarization consists of photons with spin parallel (antiparallel) to the propagation vector of the light. Under the electric dipole approximation, the excitation operator of the σ^+ light propagating in the $+z$ direction is proportional to $x + iy$, and is therefore proportional to $Y_1{}^1(\theta, \varphi)$, where $Y_\ell{}^m$ is the spherical harmonic function. A 4f electron with its magnetic quantum number ℓ_z is excited by the light with circular polarization σ^+ to the photoelectron with the magnetic quantum number $\ell_z + 1$. On the basis of our supposition that the photoelectron has $\ell' = 4$, the dependence of the photoexcitation probability is $|\int Y_4^{*(\ell_{z+1})}\, Y_1{}^1\, Y_3{}^{\ell_z}\, d\Omega|^2$, which is proportional to $(\ell_z{}^2 + 9\,\ell_z + 20)/2$, for the σ^+ excitation. The ratio of this probability is calculated to be $28 : 21 : 15 : 10 : 6 : 3 : 1$ for $\ell_z = 3, 2, 1, 0, -1, -2, -3$. This result indicates that 4f electrons with positive ℓ_z are preferentially photoexcited by the σ^+ circularly polarized light.

We assume, for simplicity, that the ground state of the $4f^6$ state is represented by $^7F_0$, whose total angular momentum is $J = 0$. Then, the total angular momentum of the final state should be the same as the angular momentum of the photoexcited hole j. When the final state is $^6H_{5/2}$, a 4f electron with $j = 5/2$ is photoexcited. There are six $j = 5/2$ states with magnetic quantum numbers of $j_z = -5/2$, $-3/2$, $-1/2$, $1/2$, $3/2$, and $5/2$, with the wave function

$$|j = 5/2, j_z\rangle = [(7 - 2j_z)/14]^{1/2} \cdot Y_3{}^{j_z - 1/2}(\theta, \varphi)\uparrow - [(7 + 2j_z)/14]^{1/2} \cdot Y_3{}^{j_z + 1/2}(\theta, \varphi)\downarrow, \quad (1)$$

where $\uparrow$ and $\downarrow$ are the up and down spin functions, respectively. Then, the wave function of the photoelectron becomes $Y_4{}^{j_z+1/2}(\theta, \varphi)\uparrow$ or $Y_4{}^{j_z+3/2}(\theta, \varphi)\downarrow$ for the σ^+ or σ^- excitation with probability proportional to

$$\{(7 - 2j_z)/14\}\{(j_z - 1/2)^2 + 9(j_z - 1/2) + 20\}, \quad (2)$$

and

$$\{(7 + 2j_z)/14\}\{(j_z + 1/2)^2 + 9(j_z + 1/2) + 20\}, \quad (3)$$

respectively. The probability of finding the electron with wave function $Y_{\ell'}{}^{\ell_{z'}}(\theta, \varphi)$ in the present experimental geometry is

$$|Y_{\ell'}{}^{\ell_{z'}}(50^\circ, 0^\circ)|^2. \quad (4)$$

Taking these factors into account, the spin polarization averaged over the six $j = 5/2$ 4f states with $j_z = -5/2, \ldots, 5/2$ excited by the σ^+ light becomes -0.43. Therefore, the $^6H_{5/2}$ peak is expected to have a spin polarization of -0.43 for fully polarized σ^+ light excitation. Similar calculation leads to spin polarization of the $^6H_{7/2}$ peak of $+0.32$.

Now, let us more realistically consider that the ground state is a Kondo state consisting of both f^5 and f^6 states. There are two possible Kondo states, namely, f^6+$f^5\underline{L}$ and f^5+$f^6\underline{L}$. Here, L ($\underline{L}$) represents an electron (a hole) in the ligand electronic orbital. According to a preliminary calculation using the Xtls code,[21] the f^6+$f^5\underline{L}$ initial state results in essentially the same spin polarization as calculated in the previous paragraph. On the other hand, the f^5+$f^6\underline{L}$ initial state results in a much smaller spin polarization. Therefore, we consider that the present experimental results indicate that the Kondo state realized in this system is f^6+$f^5\underline{L}$.

In this scheme, spin polarization is induced along any light incidence direction on the circularly polarized light excitation due to the dipole selection rules caused by the spin–orbit interaction, and spin polarization is not expected for the excitation by the linear polarization light in agreement with the experimental results. This result demonstrated that the spin-polarized Dirac cone state is not observed in the spectra obtained in this experiment. In other words, completely linear polarization light excitation or fully unpolarized light excitation is inevitable to check the presence or absence of the Dirac cone state with intrinsic spin polarization in SmB_6 at low temperatures in the E_B region within 20 meV from E_F, where an energy resolution better than 10 meV may be required for measurements. Since the low detection efficiency of single-channel spin detection cannot overcome the time-dependent surface quality change, a higher-efficiency spin detector will be inevitable in addition to realizing the best quality ultrahigh vacuum condition to acquire a complete set of information on two-dimensional spin polarization.

6. Conclusions and Prospect

As demonstrated in the present experiment, the gradual change in the surface quality with time induces a serious change in the spectral shape in the surface-sensitive low-$h\nu$ photoemission at $h\nu = 35$ eV in the E_B region between E_F and 2 eV, where most interesting surface states are expected to exist in this strongly correlated electron system, SmB_6. As experimentally revealed, the structures near E_B of ~12–20 and ~150–180 meV survive even after the change of surface quality and are thought to reflect the bulk electronic states dominated by the 4f $^6H_{5/2}$ and $^6H_{7/2}$ components at $h\nu =$ 35 eV hybridized with the B 2sp and Sm 5d states. The entire results of the spin-polarized and angle-resolved spectra obtained here are consistently understood by considering the dipole selection rules for these states by the circularly and linearly polarized light excitation. The non-observation of the spin polarization of the proposed Dirac cone state[6,7] in the present experiment may be due to either the change in the surface quality with time or the different origins of the surface metallic states. To study the spin polarization of the possible Dirac cone states in this surface sensitive material, short measuring time of SP-ARPES in two-dimensional k space under a very high quality ultrahigh vacuum as well as the use of fully linearly polarized or unpolarized light will be inevitable in addition to very high energy resolution better than 10 meV. If ellipsoidal light is employed, it may induce the spin polarization of the $^6H_{5/2}$ states obscuring the possible spin polarization of weak and tiny Dirac cone states.

Acknowledgements

The authors (S.S. and K.S.) are much obliged to Professors M. Taniguchi and A. Kimura for their interest in this subject and general warm support for this experiment. S.S. also acknowledges Dr. C. Tusche and Professor J. Kirschner for fruitful discussions and exchange of ideas on the future direction of spin-polarized angle-resolved photoelectron spectroscopy of general solid state materials.

*ssmsuga@gmail.com
†Present address: Nagoya University Synchrotron Radiation Research Center and Graduate School of Engineering, Nagoya University, Nagoya 464-8603, Japan.
‡Present address: Graduate School of Frontier Biosciences, Osaka University, Suita, Osaka 565-0871, Japan.

1) A. Menth, E. Buehler, and T. H. Geballe, Phys. Rev. Lett. **22**, 295 (1969).
2) S. Nozawa, T. Tsukamoto, K. Kanai, T. Haruna, S. Shin, and S. Kunii, J. Phys. Chem. Solids **63**, 1223 (2002).
3) F. Iga, N. Shimizu, and T. Takabatake, J. Magn. Magn. Mater. **177–181**, 337 (1998).
4) B. Gorshunov, N. Sluchanko, A. Volkov, M. Dressel, G. Knebel, A. Loidl, and S. Kunii, Phys. Rev. B **59**, 1808 (1999).
5) J. Yamaguchi, A. Sekiyama, M. Y. Kimura, H. Sugiyama, Y. Tomida, G. Funabashi, S. Komori, T. Balashov, W. Wulfhekel, T. Ito, S. Kimura, A. Higashiya, K. Tamasaku, M. Yabashi, T. Ishikawa, S. Yeo, S.-I. Lee, F. Iga, T. Takabatake, and S. Suga, New J. Phys. **15**, 043042 (2013).
6) M. Dzero, K. Sun, V. Galitski, and P. Coleman, Phys. Rev. Lett. **104**, 106408 (2010).
7) T. Takimoto, J. Phys. Soc. Jpn. **80**, 123710 (2011).
8) S. Souma, H. Kumigashira, T. Ito, T. Takahashi, and S. Kunii, Physica B **312–313**, 329 (2002).
9) H. Miyazaki, T. Hajiri, T. Ito, S. Kunii, and S. Kimura, Phys. Rev. B **86**, 075105 (2012).
10) J. Jiang, S. Li, T. Zhang, Z. Sun, F. Chen, Z. R. Ye, M. Xu, Q. Q. Ge, S. Y. Tan, X. H. Niu, M. Xia, B. P. Xie, Y. F. Li, X. H. Chen, H. H. Wen, and D. L. Feng, arXiv:1306.5664v1. ARPES was performed on (001) cleaved surfaces at SSRL, BESSYII, and HiSOR in addition to the use of a He-Iα light.
11) N. Xu, X. Shi, P. K. Biswas, C. E. Matt, R. S. Dhaka, Y. Huang, N. C. Plumb, M. Radovic, J. H. Dil, E. Pomjakushina, A. Amato, Z. Salman, D. McK. Paul, J. Mesot, H. Ding, and M. Shi, arXiv:1306.3678v1. ARPES was performed on cleaved surfaces in the $h\nu$ region from 22 to 110 eV at Swiss Light Source.
12) M. Neupane, N. Alidoust, S.-Y. Xu, T. Kondo, D.-J. Kim, C. Liu, I. Belopolski, T.-R. Chang, H.-T. Jeng, T. Durakiewicz, L. Balicas, H. Lin, A. Bansil, S. Shin, Z. Fisk, and M. Z. Hasan, arXiv:1306.4634v1. High energy resolution ARPES was performed at ISSP, The University of Tokyo by use of ~7 eV laser with the total energy resolution of 4 meV and temperature down to 6 K beside the use of synchrotron radiation at SRC, Wisconsin.
13) J. Kessler, *Polarized Electrons, Springer Series on Atoms and Plasmas* (Springer, Berlin, 1985).
14) J. Kirschner, *Polarized Electrons at Surfaces, Springer Tracts in Modern Physics* (Springer, Berlin, 1985).
15) T. Okuda, Y. Takeichi, Y. Maeda, A. Harasawa, I. Matsuda, T. Kinoshita, and A. Kakizaki, Rev. Sci. Instrum. **79**, 123117 (2008).
16) T. Okuda, K. Miyamaoto, H. Miyahara, K. Kuroda, A. Kimura, H. Namatame, and M. Taniguchi, Rev. Sci. Instrum. **82**, 103302 (2011).
17) J. J. Yeh and I. Lindau, At. Data Nucl. Data Tables **32**, 1 (1985).
18) J. Yamaguchi, A. Sekiyama, S. Imada, A. Higashiya, K. Tamasaku, M. Yabashi, T. Ishikawa, T. Ito, S. Kimura, F. Iga, T. Takabatake, S. Yeo, S.-I. Lee, H.-D. Kim, and S. Suga, J. Phys.: Conf. Ser. **200**, 012230 (2010).
19) Z.-H. Zhu, A. Nicolaou, G. Levy, N. P. Butch, P. Syers, X. F. Wang, J. Paglione, G. A. Sawatzky, I. S. Elfimov, and A. Damascelli, arXiv:1309.2945v1. ARPES was measured at $h\nu = 21.2$ eV and 6 K on cleaved surfaces.
20) S. M. Goldberg, C. S. Fadley, and S. Kono, J. Electron Spectrosc. Relat. Phenom. **21**, 285 (1981).
21) A. Tanaka, T. Jo, and G. A. Sawatzky, J. Phys. Soc. Jpn. **61**, 2636 (1992).